Talanta 215 (2020) 120909

Contents lists available at ScienceDirect

Talanta

journal homepage: www.elsevier.com/locate/talanta

Highly sensitive impedimetric immunosensor for determination of interleukin 6 as a cancer biomarker by using conjugated polymer containing epoxy side groups modified disposable ITO electrode

Elif Burcu Aydın

Tekirdağ Namık Kemal University, Scientific and Technological Research Center, Tekirdağ-Turkey

ARTICLE INFO

Keywords:
Interleukin 6
Pyrrole-based conjugated polymer containing epoxy active side groups
Impedimetric immunosensor
Prostate cancer

ABSTRACT

A novel impedimetric immunosensor based on a conjugated polypyrrole polymer containing epoxy active side groups (PPCE) modified indium tin oxide (ITO) electrode was developed for detection of interleukin 6 (IL 6), a prostate cancer biomarker. IL 6 receptor was used as a biorecognition molecule and successfully immobilized by covalent linkage on the modified ITO electrode. Pyrrole monomer containing epoxy active side group was electropolymerized on the disposable ITO electrode for the first time and used as an immobilization matrix for IL 6 receptor. The designed biosensor fabrication stages were analyzed by using electrochemical impedance spectroscopy (EIS) and cyclic voltammetry (CV) techniques. For the quantification of IL 6 biomarker, EIS technique was utilized. In addition, the specific immuno-interaction between IL 6 receptor and IL 6 antigen was followed by single frequency impedance (SFI) technique. The resulting biosensor exhibited a linear calibration curve over the 0.02–16 pg/mL IL 6 concentration range, a limit of detection (LOD) of 6.0 fg/mL and a good selectivity against other interference biomarkers. Additionally, an excellent reproducibility, a long storage stability and an acceptable repeatability were found. The proposed impedimetric immunosensor was applied successfully to quantify for the IL 6 biomarker in human serum and it displayed a remarkable response in the real sample analysis with serum samples. In comparison with the commercial ELISA kit, the immunosensor provided a lower LOD and a lower analysis cost. In conclusion, the proposed impedimetric immunosensor could be clinically useful in the early diagnosis of the prostate cancer by detection of the serum samples after only simple dilution with phosphate buffer.

1. Introduction

Prostate cancer (PCa) is deadly malignancy which forms in the outermost part of prostate due to mutation of DNA. PCa leads to uncontrolled proliferation, differentiation and in the next times it causes metastasis in different organs [1]. In addition, PCa is a major cause of death in men aged between 50 and 80 years[1–3]. The early detection of prostate cancer is difficult and mortality rates increase each year. Ultrasonography, digital rectal inspection, computed tomography scan, magnetic resonance imaging and cancer protein assay are the mostly used PCa detection methods [4].

Biomarkers are indicators which identify any biological states or conditions in the living body [5,6]. The origins of biomarkers are DNA and RNA proteins, DNA modifications and DNA metabolites [1,7]. PCa biomarkers are typically measured in blood or serum and urine samples [8,9]. Prostate specific antigen (PSA) is the best-known serum cancer biomarker, which is usually utilized in nowadays for the diagnosis of PCa disease and clinical finding illustrates that PSA serum concentrations higher than 4.0 ng/mL are abnormal [10–14]. However, in some cases such as prostatic hyperplasia, prostatitis, benign prostate hyperplasia or cystitis, the level of PSA increases, and this increase causes a false positive result [11]. Therefore, a new prostate cancer biomarker is demand for PCa detection.

Interleukin 6 (IL 6) is a multifunctional cytokine that affects the cancer cells activity [15,16]. IL 6 is a 26 kDa glycoprotein and it includes 184 amino acids. IL 6 is produced by monocytes, macrophages, lymphocytes, fibroblasts, keratinocytes, endothelial cells and some tumor cells [17,18]. It induces growth and differentiation of B cells, secretion of immunoglobulins, activation of T cells and acute phase response of proteins [19,20]. Many diseases including osteoarthrosis, asthma, psoriasis, cardiovascular disease, diabetes and inflammatory bowel disease are closely associated with IL-6 and these diseases can increase the IL-6 concentration in human serum [21–23]. In addition, it is an important biomarker overexpressed by several types of cancer

E-mail addresses: bebahadir@hotmail.com, ebbahadir@nku.edu.tr.

https://doi.org/10.1016/j.talanta.2020.120909
Received 20 January 2020; Received in revised form 4 March 2020; Accepted 7 March 2020
Available online 12 March 2020
0039-9140/

including prostate cancer [20]. In healthy individuals, it is present at a very low level around 6 pg/mL in human serum, making the earlier diagnosis of diseases via detecting this biomarker a rather challenging task [24]. Because of this, it is very important to develop new technologies for determination of IL 6 level in human biological fluids. The accurate determination of IL 6 level provides rapid diagnosis of disease and also effective monitoring of subsequent therapy [24]. The present traditional techniques for IL6 cancer biomarker detection are radioimmunoassay, chemiluminescence immunoassay, enzyme-linked immunoassay (ELISA), fluoroimmunoassay and electrophoretic immunoassay [18,22,23]. All these methods require expensive instrument, well-controlled experimental conditions and specialized personnel. Contrary to these techniques, electrochemical biosensors have become the predominant technique due to their high sensitivity, simple instrumentation and excellent compatibility with miniaturized technologies. In this context, in recent years, electrochemical immunosensors are usually used for cancer biomarker detection because of their advantages such as high sensitivity and low detection limit [25,26].

In order to detect cancer biomarkers properly in any biological fluids, electrode surface preparation is an important stage for immunosensor fabrication [27]. Different analytical applications of conjugated polymers in the area of biomedical applications and biosensing systems have been reported since their discovery [28]. Conjugated polymers (CPs) are flexible in chemical structure and also, they can be modified easily. It is possible to modulate the required electronic and mechanical features of conjugated polymers by chemical reactions. CPs have gained attention as suitable matrices for biomolecules immobilization and they can be utilized to enhance stability and sensitivity of the biosensor [29]. The most important advantage of conjugated polymer-based biosensors over other analytical techniques is that the improved response feature and sensitivity to small perturbations [30]. CPs modified biosensors provide simple, accurate, reliable and low-cost detection of various analytes and act as effective analytical tools. Furthermore, their biocompatibility and sufficient stability make them excellent immobilization matrices for biomolecule immobilization. Many techniques such as physical adsorption, electrochemical entrapment and covalent binding have been employed to improve the stability of the biosensor [28]. Biomolecules, such as enzymes, receptors, DNAs, aptamers and antibodies can be attached onto CPs without any loss of their activity, which makes CPs as a biocompatible material for biological molecule immobilization. Polypyrrole (PPy) is mostly utilized CP in the development of biosensors because of its good biocompatibility, considerable conductivity, high stability and efficient polymerization [30,31]. Moreover, PPy is a suitable interface material and the PPy film formation on the electrode surface makes it possible to introduce functional groups on the electrode surface. Additionally, PPy film increases electrode surface area owing to its ramified polymer network and it is stable at ambient conditions. Moreover, it provides an easy way to immobilize biomolecules and also, it prevents enzymes from leaching out of the biocatalytic layer [32]. In recent years, a lot of enzyme biosensors [33,34] immunosensors [31,35], DNA biosensor [36,37] have utilized PPy as a suitable matrix.

Given the fact that the early detection of IL 6 antigen in prostate cancer patients could provide a useful disease treatment, in this study, a highly sensitive, low-cost and simple impedimetric immunosensor was developed for the determination of IL 6 antigen. In the proposed immunosensor, disposable ITO electrodes were employed as electrochemical transducers. Because of the low electrochemical conductivity of biological molecules, ITO was a desirable material considering its low surface resistivity, chemical stability, wide electrochemical working area and stable electrochemical features. Furthermore, ITO allowed biochemical modification and it was suitable for biosensing applications. In addition, ITO was chosen instead of a carbon-based electrode due to its low cost. The biorecognition molecules, interleukin 6 receptors, were implemented onto a conjugated polypyrrole polymer containing epoxy active side groups (PPCE) modified ITO electrode. PPCE was a novel conjugated polymer matrix and coated on the disposable ITO electrode via electropolymerization of pyrrole monomer containing epoxy active side group (PCE). In this work, PCE monomer was synthesized to prepare a low-cost and conductive interface material and applied for IL 6 receptors immobilization because the epoxy groups present on the PPCE polymer provided attachment points for covalent binding of receptors. The biocompatibility and good stability of the PPCE polymer made it an excellent immobilization matrix for IL 6 receptor immobilization and it provided a more efficient charge transfer between receptor and the ITO electrode surface. IL 6 receptors attached on the ITO electrode via covalent binding between amino groups of receptor and epoxy groups of polymer PPCE. Specific biointeractions between IL 6 receptors and IL 6 antigens were confirmed EIS, CV and SFI measurements. The step-by-step modification process was also investigated by scanning electron microscopy (SEM) and atomic force microscopy (AFM) analyses. The proposed immunosensor was successfully used in serum samples for IL 6 antigen determination.

2. Experimental

2.1. Reagents

1-(2-Cyanoethyl)pyrrole (Pyr-CN, 99%), potassium hydroxide (KOH, 99%), 4-dimethylamino pyridine (DMAP, ≥99%), 1-ethyl-3-(dimethyl-aminopropyl) carbodiimide hydrochloride (EDC), tetrahydrofuran (THF, ≥99.5%), hydrochloric acid (HCl, 37%), glycidol (GOH, 96%) and diethyl ether (≥99%) tetrabutylammonium chloride (≥99%) were purchased from Sigma-Aldrich (USA). Potassium chloride (KCl), potassium dihydrogen phosphate (KH_2PO_4), dipotassium hydrogen phosphate (K_2HPO_4), potassium ferrocyanide (K_4 [Fe $(CN)_6$]) and potassium ferricyanide (K_4 [$Fe(CN)_6$]) were utilized for phosphate buffer solution and ferri/ferrocyanide redox couple solution preparation and were obtained from Sigma-Aldrich (USA). Indium tin oxide coated polyethylene terephthalate film (ITO-PET) electrodes (0.5 cm × 2 cm, 60 Ω/cm2, Sigma-Aldrich), IL 6 receptor (Soluble fragment human 25 μg), IL 6 antigen (human, 10 μg) and bovine serum albumin (BSA) were from Sigma-Aldrich (USA). The blocking agent was a commercial BSA solution (0.5%) prepared in 50 mM PBS buffer (pH 7.4). All solutions used in this study were prepared with ultrapure water obtained from Elga Purelab OptionQ Ultrapure Water system (18.2 MΩ). Vascular endothelial growth factor (VEGF), protein p53 (p53), interleukin 8 (IL 8) and interleukin 1β (IL 1β) biomolecules were applied as potential interfering biomolecules.

2.2. Instrumentations

IR spectra were recorded using FTIR reflectance spectroscopy in the range of 4000–400 cm^{-1} (Bruker, Vertex 70 spectrometer with ATR, Germany). The Raman spectra were recorded using DXR Raman spectrometer with a 780-nm excitation laser (Thermo Scientific Company, USA). ^{1}H NMR spectra of monomers were taken by using 400 MHz Bruker Avance II (Bruker Company, Germany) using $CDCl_3$ deuterated solvents. Electrochemical measurements were performed on Gamry Reference 1000 Workstation (USA) employing a three-electrode system composed of an ITO substrate (0.5*2 cm) as a working electrode, a platinum wire as a counter electrode, and Ag/AgCl as a reference electrode. The surface morphology of the proposed biosensor was characterized by SEM, energy dispersive X-ray (QUANTA FEG-250 Field Emission Scanning Electron Microscope, FEI Company, USA) and AFM (Hp-AFM, NanoMagnetic Instrument, Turkey) devices. SEM and energy dispersive X-ray analysis were performed with a low vacuum detector. During the SEM analyses, acceleration voltage, spot size and sample-to-detector distance were 5 kV, 3.5, and 10 mm, respectively. In EDX analysis, the acceleration voltage and spot size were 30 kV and 5.5, respectively. AFM analysis of ITO sheet surface was carried out in

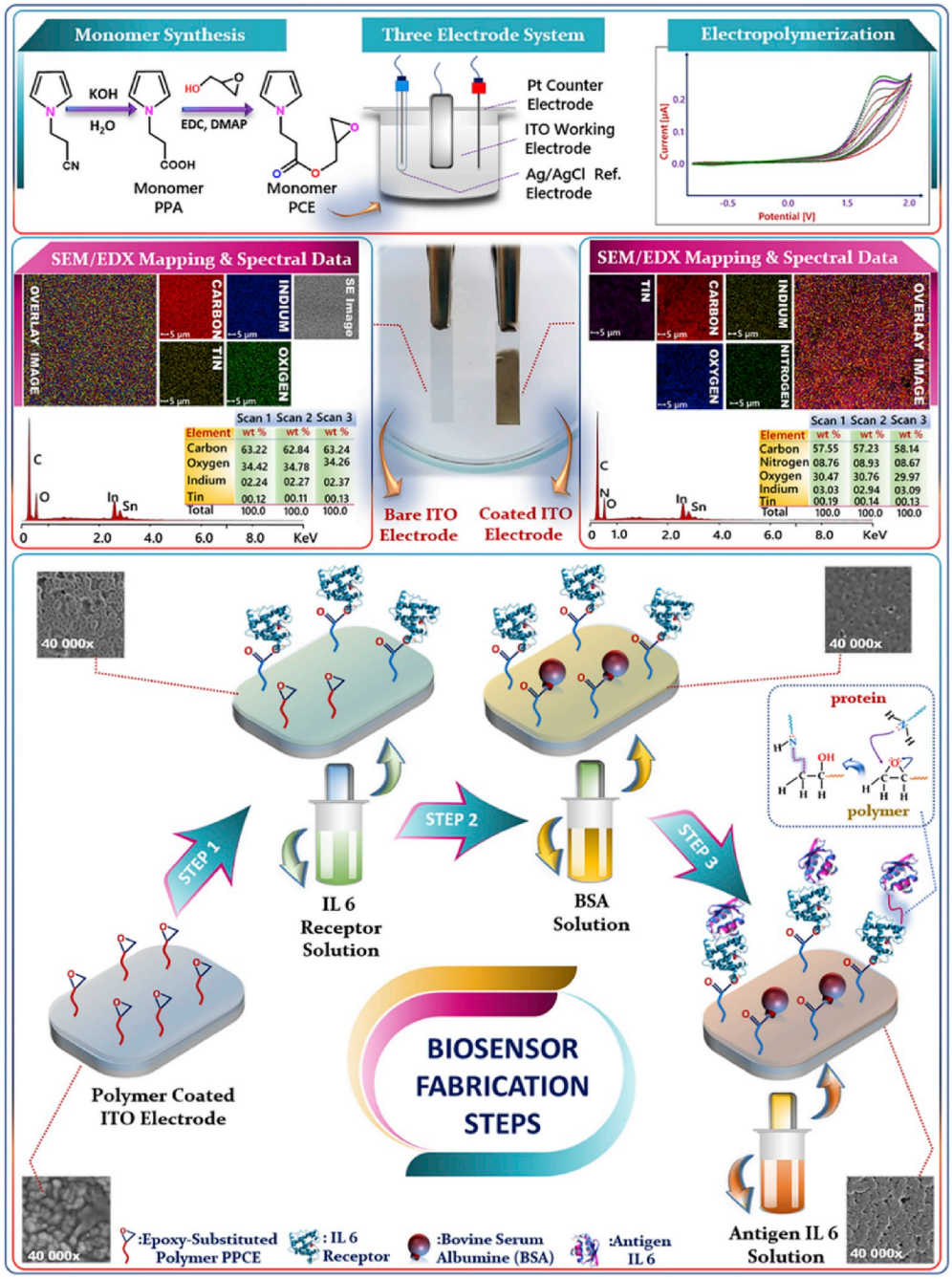

Scheme 1. Synthesis mechanism of the PCE monomer, electropolymerization cycles, EDAX elemental mapping and spectra of ITO surface before and after electropolymerization of PCE monomer, and fabrication process of the suggested immunosensor.

tapping mode. The scan rate was 2 µm/s with a resolution of 256 pixels per line. Three-dimensional (3D) AFM images were recorded utilizing NanoMagnetics image analyzer software.

2.3. Procedures

2.3.1. Synthesis of the PPA and PCE monomers

Pyrrole monomer containing acid functional groups (pyrrole-propionic acid-PPA) was synthesized to the previous reported procedures with minor modifications [38,39]. The PCE monomer was synthesized and characterized according to a previously described method [39]. In sum, pyrrole-propionic acid monomer was synthesized by alkaline hydrolysis reaction of 1-(2-cyanoethyl)pyrrole. The pyrrole monomer containing epoxy active side group (PCE) monomer was synthesized by esterification reaction of pyrrole-propionic acid and glycidol. The synthesis scheme of monomer PPA and monomer PCE is shown in Scheme 1. The chemical characterizations of monomers and the obtained results are given in supp. material part.

2.3.2. Preparation of IL 6 immunosensor

The proposed immunosensor construction procedure details are shown in Scheme 1. Before IL 6 immunosensor preparation procedure, ITO electrode was washed thoroughly with acetone, soap solution and ultrapure water in an ultrasonic bath. To prepare PPCE coated ITO electrode, PCE monomer (0.1 mg/mL) was electropolymerized on ITO electrode via 10 cycle voltammograms in the presence of 0.1 M tetrabutylammonium chloride in acetonitrile electrolyte/solvent system between the potential range +0.2 V and 2.0 V at a scan rate of 50 mV/

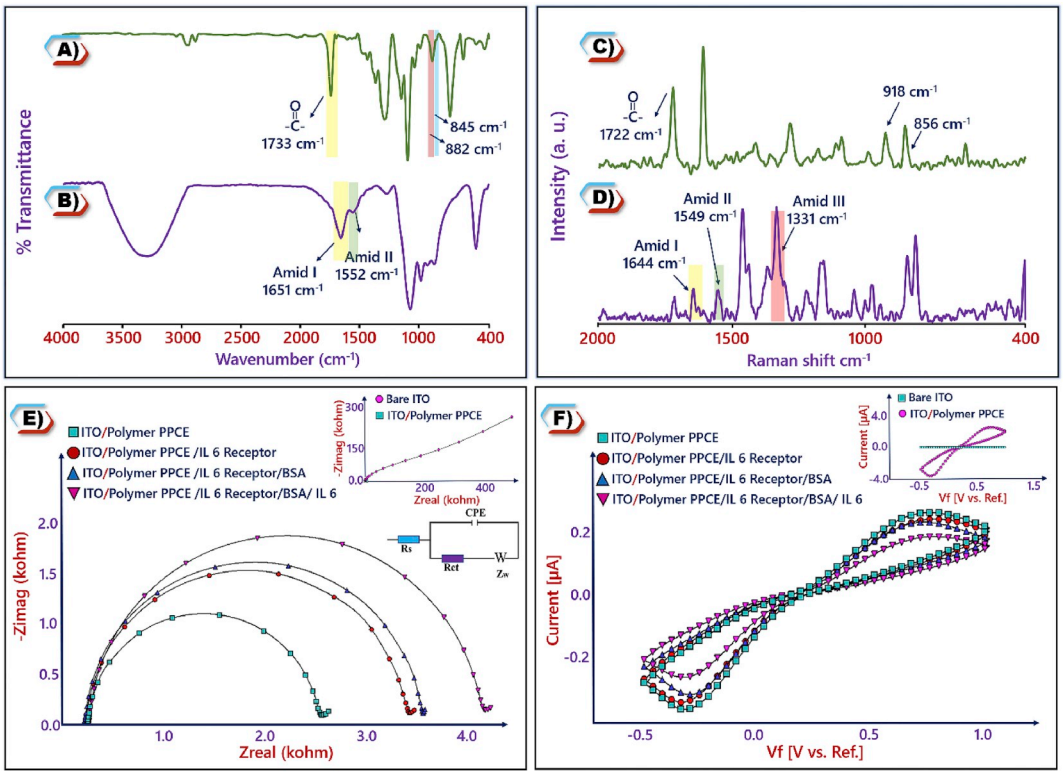

Fig. 1. FTIR spectra of ITO/PPCE (A) and ITO/PPCE/IL 6R (B); and Raman spectra of ITO/PPCE (C) and ITO/PPCE/IL 6R (D); Electrochemical impedance spectra of ITO/PPCE, ITO/PPCE/IL 6R, ITO/PPCE/IL 6R/BSA, ITO/PPCE/IL 6R/BSA/IL 6 in the frequency range from 0.5 Hz to 50,000 Hz (E); Cyclic voltammograms obtained from ITO/PPCE, ITO/PPCE/IL 6R, ITO/PPCE/IL 6R/BSA, ITO/PPCE/IL 6R/BSA/IL 6 at scan rate of 100 mVs^{-1} (F).

s. Then, polymer coated ITO electrode was rinsed with ultrapure water to remove possible impurities. After that, polymer PPCE modified ITO electrode was immersed in IL 6 receptor solution and incubated there for 45 min to obtain the ITO/PPCE/IL 6R electrode. The constructed ITO/PPCE/IL 6R electrode was washed with ultrapure water thoroughly to remove unattached or weak attached IL 6 receptors on the ITO surface. To prevent the non-specific binding, ITO/PPCE/IL 6R electrode was immersed in BSA solution for 1 h. After blockage by BSA, the ITO/PPCE/IL 6R/BSA electrode was washed with ultrapure water to remove the redundant BSA on the immunosensing surface. Finally, the ITO/PPCE/IL 6R/BSA electrode was ready to detect IL 6 antigen.

2.3.3. Electrochemical measurements

For the electrochemical characterization of the designed biosensor fabrication procedure, EIS and CV analyses were carried out after each modification process. The electrolyte solution utilized in all the electrochemical analyses contained 0.1 M KCl and 5 M $K_3Fe(CN)_6/K_4Fe(CN)_6$ (1:1), in which $[Fe(CN)_6]^{4-/3-}$ was used as the redox couple. The potentials of CV were set from −0.5 to 1 V at a scan rate of 100 mV/s. The frequency of EIS analysis was recorded from 50 kHz to 0.5 Hz. The alternating potential and formal potential applied during EIS measurements were 5 mV and 0 V, respectively. IL 6 determination was performed by using ITO/PPCE/IL 6R/BSA bioelectrode as a working electrode and the all electrochemical measurements were recorded via Echem Analyst software program.

2.3.4. Determination of IL 6 antigen

After construction of ITO/PPCE/IL 6R/BSA immunoelectrode, it was immersed in different concentrations of IL 6 antigen solution for 30 min. The EIS measurements were carried out in the electrochemical cell containing ferri-ferro solution and the obtained signals were used to determine IL6 concentration.

2.3.5. Application of the proposed immunosensor to the serum samples

Serum samples were provided by Tekirdağ Namık Kemal University, Faculty of Medicine (Ethic committee approval 2013/86/07/05). The samples were analyzed using ITO/PPCE/IL 6R/BSA immunosensor after a 10-fold sample dilution with PBS buffer.

3. Results and discussion

In this work, PPCE coated ITO electrode-based IL 6 immunosensor was designed after simple preparation steps. Firstly, PCE monomer was synthesized and electropolymerized on the ITO electrode surface. After electropolymerization of PCE monomer, the PPCE coated electrode was ready to immobilize the IL 6 receptors. Scheme 1 shows schematically synthesis mechanism of the PCE monomer and fabrication process of the ITO/PPCE/IL 6R/BSA/IL 6 immunosensor. The fabrication process included 3 steps; covalent immobilization of IL 6 receptor on the ITO/PPCE electrode (step 1), blockage the remaining free active sites with BSA (step 2) and detection of IL 6 antigen (step 3). The affinity reaction was monitored by EIS and CV techniques and the quantification of the IL 6 antigen concentration was performed by EIS analysis.

3.1. Choice of materials

Polypyrrole polymer was the most preferred conjugated polymer for biosensor fabrication. It had good environmental stability, simple synthesis and higher conductivity than other conjugated polymers. PPCE polymer had excessive epoxy active side groups and these groups bound to amino groups of IL 6 receptor covalently. This reaction did not require a crosslinker. Furthermore, this electropolymerized polymer supported the electrochemical conductivity of the electrode surface. The synthesis of PCE monomer had a low-cost synthesis procedure and the electropolymerization of PCE monomer was easy. Furthermore, the fabrication cost of the immunosensor was low thanks to the low-cost

synthesis procedure and the PPCE polymer-based immunosensor had a good performance for detection of IL 6 biomarker. As a consequence of these properties, the PPCE polymer was a unique interface material for biosensing element immobilization.

3.2. Chemical characterizations of ITO/PPCE and ITO/PPCE/IL 6R electrode surfaces

The infrared spectra of the PCE monomer electropolymerized ITO substrate surface (green line) and IL 6 receptor attached ITO substrate surface (purple line) are illustrated in Fig. 1A and B, respectively. As observed in Fig. 1A, the PCE monomer containing active epoxy group electropolymerized ITO electrode had two absorption peaks at 845 cm^{-1} and 882 cm^{-1} because of oxirane ring present on the side groups of polymer. The strong signal seen around 1733 cm^{-1} was attributed to C═O stretching vibration of carbonyl groups in repeating units [38]. After covalent immobilization of IL 6 receptor on the ITO electrode surface, broad and intense bands at around 1651 cm^{-1} (amid I) and 1552 cm^{-1} (amid II) were seen. These bands were classical protein bands, and these bands proved the attachment of the IL 6 receptor onto the PPCE polymer modified ITO substrate surface [40–43]. Apart from FTIR analysis, the chemical characterizations of polymer coated ITO substrate surface (green line) and IL 6 receptor attached ITO substrate surface (purple line) were performed by using Raman spectroscopy (Fig. 1C and D). This technique is the best complementary spectral tool to FTIR spectroscopy [44–46]. At green line in Fig. 1C, monomer electropolymerized ITO substrate surface had oxirane side group peaks at 856 cm^{-1} and 918 cm^{-1}. The Raman spectral technique is more suitable technique to identify amide bonds than FTIR technique [47]. The bands of amide I, II and III regions are seen between 1600 and 1680 cm^{-1}, 1480-1570 cm^{-1} and 1235-1350 cm^{-1}, respectively [47–49]. As shown in Fig. 1D, amide I, amide II and amide III bonds were observed at 1644, 1549 and 1331 cm^{-1}, respectively [50].

Energy-dispersive x-ray spectroscopy analysis was performed to monitor the elemental composition of bare ITO substrate and PCE monomer electropolymerized ITO substrate. As illustrated in Scheme 1, bare ITO had carbon (C), oxygen (O), indium (In), and tin (Sn) elements and this finding was compatible with other research results [51,52]. After electropolymerization process, spectra had carbon (C), oxygen (O), nitrogen (N), indium (In), and tin (Sn) elements. The presence of N atom in the spectra indicated that the monomer was successfully electropolymerized on the ITO sheet surface and these N atoms were from PPCE polymer. Moreover, when the bare and polymer coated ITO electrodes in Scheme 1 were compared, the color difference between the electrodes was further evidence that the electropolymerization process was successful. The nitrogen atom ratios of 3 different regions on the ITO electrode surface were found as 8.76%, 8.93% and 8.67%. These similar ratios indicated that the PPCE polymer was homogenous coated on the ITO surface. These results illustrated that PCE monomer was electropolymerized effectively on the ITO substrate surface.

3.3. Electrochemical characterization of the proposed biosensor construction stages

The fabrication stages of the designed biosensor were evaluated by CV and EIS techniques using the electrochemical redox probe, $K_3Fe(CN)_6/K_4Fe(CN)_6$ (1:1) (5 mM) and KCl (0.1 M). Fig. 1E shows the impedance response of each step in the stepwise modification of electrodes. The impedance spectra contain a semicircle part at high frequencies corresponding to the electron transfer limited process and a linear part at low frequencies corresponding to diffusion limiting step of the electrochemical process. The diameter of semicircle equals to electron transfer resistance (R_{ct}) that shows the blocking behavior of the electrode surface for redox couple. Therefore, the change in R_{ct} gives an information about the modification process. The impedimetric signals of a biosensor is fitted by using the Randle's equivalent circuit (inset Fig. 1E), which contains the electrolyte solution resistance (R_s), the charge transfer resistance (R_{ct}), the constant phase element (CPE) and Warburg impedance (W) [52,53]. As seen in Fig. 1E, the formation of PPCE polymer layer on the ITO electrode acted as an insulating layer which had a small R_{ct}. After IL 6 receptor immobilization, a significant increase in R_{ct} was obtained and it proved the successful binding of receptor on the polymer coated electrode. Since the biomolecules were low conductors, they generated a protein layer that blocked electron transfer. In this step, amino groups of IL 6 receptor bound to epoxy groups of polymer via ring opening reaction [54]. The elimination of free epoxy groups by BSA coupling caused an increase in R_{ct} value. This increase in R_{ct} value was originated from the generation of an insulating protein layer on the ITO electrode. The formed protein layer blocked the redox probe diffusion toward electrode. Following this, the IL 6 antigen immobilization on the ITO electrode surface caused an increase in R_{ct} value because of a nonconductive protein immunocomplex formation on the electrode surface. The increase in semicircle diameter proved the hindrance of the electron flow. These results confirmed that the IL 6 sensitive immunosensor was successfully fabricated. Fig. 1F displays the CVs of four different electrodes; ITO/PPCE, ITO/PPCE/IL 6R, ITO/PPCE/IL 6R/BSA, ITO/PPCE/IL 6R/BSA/IL 6. As presented in Fig. 1F, the CV of PPCE monomer electropolymerized ITO electrode had small peak currents. Immobilization of IL 6 receptor, BSA and IL 6 antigen on the electrode surface caused decreases in oxidation and reduction peaks of CVs due to the insulating character of the biological molecules. The decreases confirmed the success of biomolecules immobilization on the electrode surface.

3.4. Electrode surface characterization by SEM and AFM

The surface morphology of the designed immunosensor was elucidated by SEM and AFM images. Fig. 3 displays the scanning electron microscopic and atomic force microscopic top views of the four modified electrodes at twenty thousand multiples. Fig. 2A and B illustrate the SEM and AFM images of PCE monomer electropolymerized ITO electrode surface and as seen in these images, a homogenous polymer layer was formed on the ITO electrode surface. In addition, a dense polymer layer was coated completely on the ITO electrode surface to provide a surface area for IL 6 receptor immobilization. The average roughness (R_a) of the PCE monomer electropolymerized ITO sheet was 18.5 nm. Fig. 2C and D showed ITO electrode surface immobilized with IL 6R receptors and the ITO electrode surface was varied completely after IL 6R receptors attachment. The R_a of the receptor immobilized ITO surface was 37.6 nm. The increase in R_a proved successful immobilization of IL 6 receptors. After blockage of free epoxy groups by BSA, the surface of electrode looked smooth (Fig. 2E and F) and a decrease was seen in R_a value (16.9 nm). As seen in Fig. 2G and H, the surface morphology of the ITO surface was changed, and an increase was seen in R_a because of IL 6 antigen immobilization. The electrodes immobilized with IL 6R receptor and IL 6 antigen indicated larger clusters owing to macro-biomolecule on the surface as presented in Fig. 2C and G. The R_a of the IL 6 antigen immobilized ITO sheet was 67.6 nm. Thus, the SEM and AFM images clearly displayed the changes in the surface morphology of the electrode and also confirmed the attachment of IL 6 receptors and IL 6 antigens on the ITO substrate surface.

3.5. Optimization of the experimental conditions during the immunosensor fabrication

To obtain a reproducible and stable IL 6 biosensor, several parameters, which might affect the sensitivity of immunosensor, were optimized. The optimized parameters are: scan cycles for polymer layer coating, IL 6 receptor concentration and incubation duration, and IL 6 antigen incubation duration. The highest immunosensor response was taken as the selection criterion for each tested variable. The results of

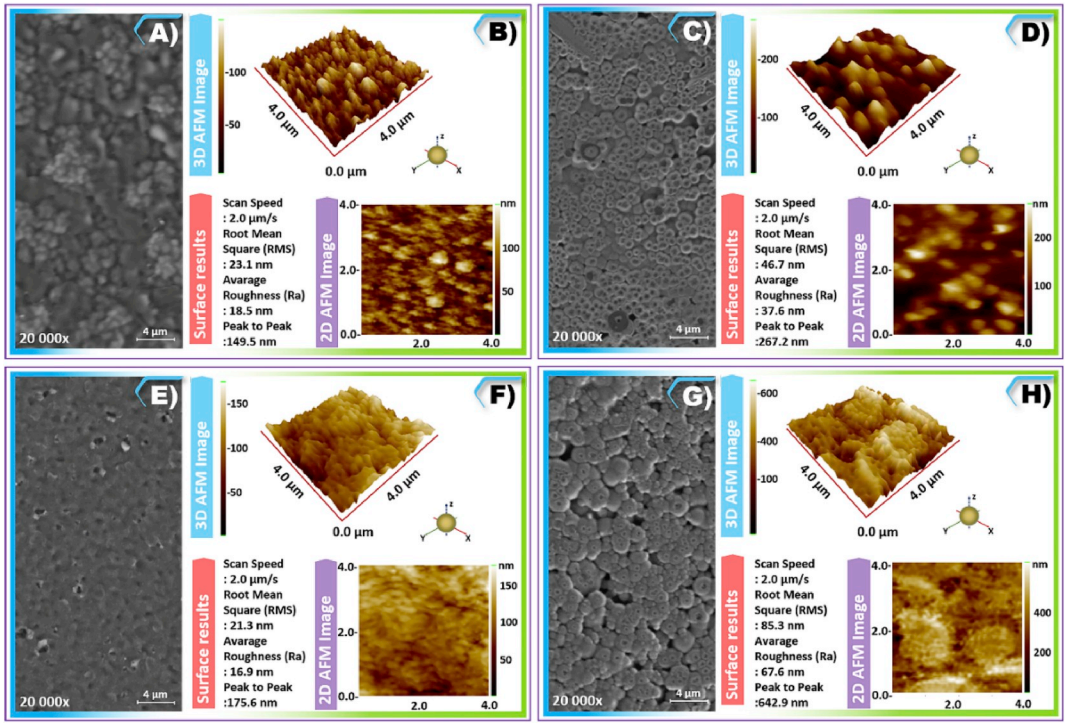

Fig. 2. SEM and AFM images of ITO/PPCE (A and B), ITO/PPCE/IL 6R (C and D), ITO/PPCE/IL 6R/BSA (E and F), ITO/PPCE/IL 6R/BSA/IL 6 (G and H).

the optimization experiments are given in Fig. 3. During the optimization and analytical characterization experiments, the used IL 6 antigen levels were 0.02 pg/mL, 0.1 pg/mL, 0.5 pg/mL, 1 pg/mL, 2 pg/mL, 4 pg/mL, 8 pg/mL and 16 pg/mL. The impedimetric responses of the designed biosensor were recorded after incubation in these antigen solutions and calibration curves were obtained after repeating 3 times the related experiments.

At the first optimization step, the thickness of polymer employed in the immunosensor fabrication procedure was optimized. The optimum polymer thickness was determined by deposition of PPCE polymer on the ITO electrode surface with scans between 5, 10 and 25 cycles. The thickness of polymer film can be controlled during polymerization process in terms of charge passing through the cell. The thickness of the polymer layer was important directly for formation of a stable conducting polymer layer in fabrication of the immunosensor. If the layer was too thick, the electron transfer between the electrode surface and

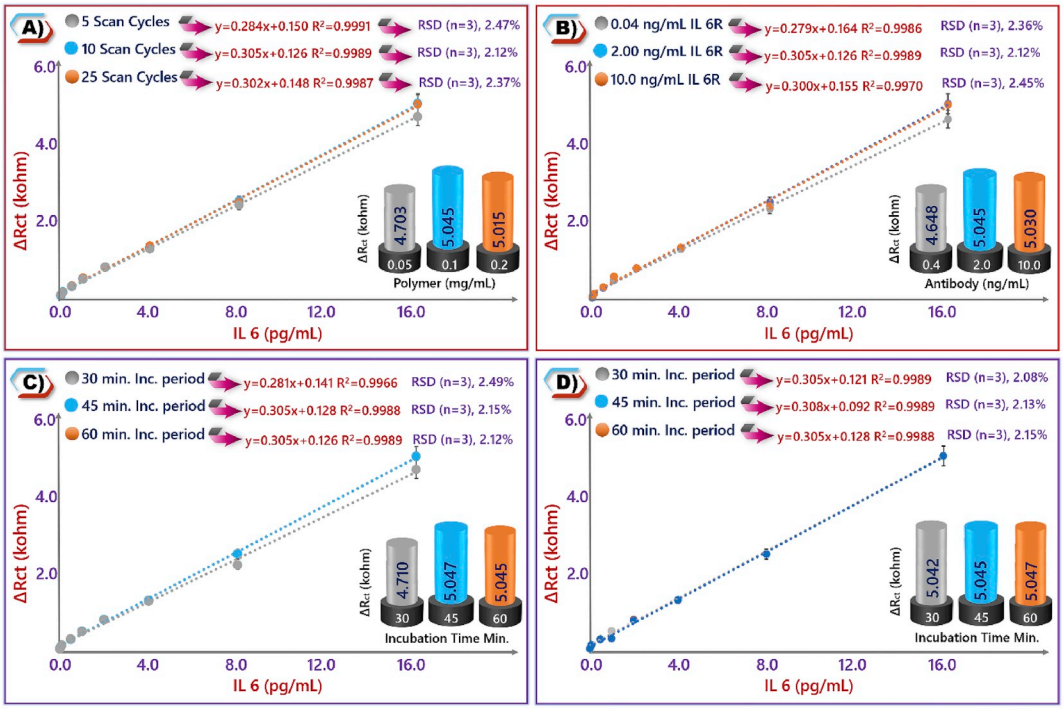

Fig. 3. Optimization studies and results of scan cycles for PPCE polymer coating (A), IL 6R receptor concentration (B), IL 6 receptor incubation period (C), IL 6 antigen incubation period (D).

electrode solution was hindered and, therefore, a high R_{ct} value was obtained. On the contrary, if the layer was too thin, the enough amount of biomolecule could not bind to the electrode surface and that caused a low biosensor response. As seen in Figs. 3A and 10 scan cycles provided optimum thickness for the biosensor. Because of this, the ITO electrode coated with 10-cycle showed a high signal arranging excellent immobilization structure and employed for subsequent studies (Fig. 3A).

In another experiment, the effect of receptor concentration on the immunosensor response was examined. Based on Fig. 3B, with increasing the receptor concentration, the immunosensor response was increased. In low concentration of IL 6 receptor (0.4 ng/mL), a sufficient response was not obtained. When used IL 6R receptor level was 10 ng/mL, the impedimetric response was a bit lower than the signal after incubation in 2 ng/mL IL 6 receptor solution. Therefore, 2 ng/mL was selected as optimal receptor level. The incubation period of IL 6 receptor used for covering the epoxy groups of polymer on the immunosensor surface affected the immunosensor performance. The ITO/PPCE electrodes were separately incubated in receptor solution for different times and used for IL 6 detection. A low impedimetric response was observed after 30 min incubation in PBS containing IL 6 receptor. The highest impedimetric signal was obtained after 45 min-incubation. Therefore, 45 min was chosen as the optimal receptor incubation period (Fig. 3C). The receptor-antigen interaction period was another important parameter that affect the success of the biosensor. The ITO/PPCE/IL 6R/BSA electrodes were incubated for various time (30–60 min) in PBS solution containing IL 6 antigen. The impedimetric responses were similar after 30 min and 45 min incubation. Therefore, 30 min was sufficient incubation period for measuring IL 6 antigen (Fig. 3D).

3.6. Analytical performance of engineered immunosensor for quantification of IL 6

The analytical performance of the designed biosensor was studied utilizing the EIS and CV techniques under the optimum analysis conditions in the presence of various concentrations of IL 6 antigen. Fig. 4A and B shows the EIS spectra and CVs after immobilization of different concentrations of IL 6 antigen from 0.02 to 16 pg/mL. The obtained peak currents and Nyquist plots illustrated that increasing IL 6 concentrations led to increases in the impedimetric responses and decreases in peak currents of the prepared biosensor. In other words, under the optimum conditions, there was a relationship between the level of IL 6 antigen and the impedance response. The linear relationship of IL 6 biosensor response could be illustrated by the equation of $\Delta R_{ct} = 0.306\ [IL\ 6] + 0.135$ with a coefficient correlation of 0.999 (Fig. 4C). The limit of detection (LOD) of 6.0 fg/mL was calculated according to the signal to noise ratio (3σ; σ is the standard deviation of the blank, n = 5). The limit of quantification (LOQ) and sensitivity were calculated as 21.5 fg/mL and 1.28 $pgmL^{-1}kohm^{-1}cm^{-2}$, respectively.

Single impedance frequency technique is used for the measurement of impedance of the system at a single frequency. In this technique, electrochemical impedance is measured versus time during the changes continued on the electrode surface [55,56]. In this work, this method was employed for following of specific immuno-interaction between IL 6 receptors and IL 6 antigens. The single frequency (12 Hz) was obtained from Bode plot (Figure SI-4) because Nyquist plot did not contain frequency data. The SFI measurement was performed in an electrochemical cell containing IL 6 antigen (2 pg/mL) and PBS buffer. During this experiment, an increase was obtained in impedance value. The increase in the impedance was an evidence of specific bio-interaction (Fig. 4D).

A comparison among the present IL 6 biosensors reported in literature and other IL6 detection methods are summarized in Table 1A. Table 1A illustrated that our proposed biosensor had an excellent limit of detection compared to other sensors designed for detection of IL 6. The usage of the polymer matrix provided simple, sensitive and low-cost biosensor development. Additionally, the proposed biosensor could detect the IL 6 concentration in shorter time than ELISA.

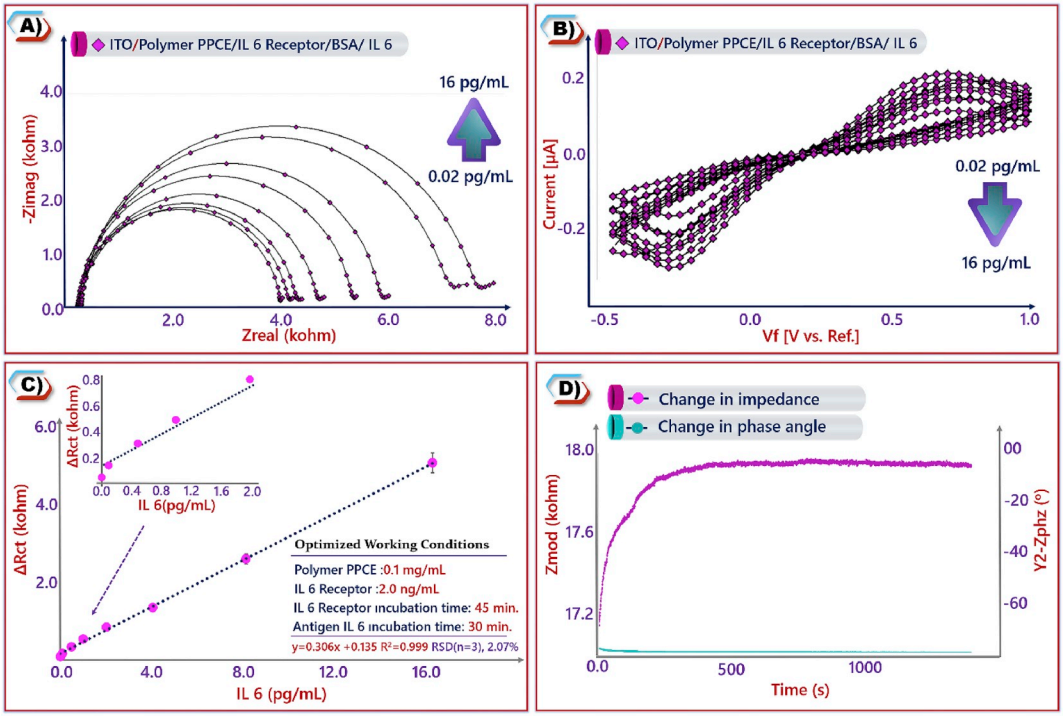

Fig. 4. Nyquist plots (A) and cyclic voltammograms (B) obtained from the designed immunosensor with increases in IL 6 antigen concentration from 0.02 to 16 pg/mL, the calibration curve obtained from the EIS responses between 0.02 and 16 pg/mL (C) and SFI result of system (D).

Table 1
A comparison of the performance of several IL 6 detection techniques (A), Determination of IL 6 antigen in human serum samples (B).

A) Detection Technique	Methods	Linear Detection Range (pg/mL)	Detection Limit (pg/mL)	Ref.
Photoelectrochemical	TiO_2/CdS/CdSe photoelectrochemical immunoassay	1–10^5	0.38	[22]
Surface-enhanced Raman scattering	SERs based lateral flow assay (LFA)	1–10^6	1	[15]
Electrochemical	AuNPs/single walled carbon nanotubes (SWCNTs) modified SiO_2/Si substrate	10^{-5}–10^{-1}	0.1	[57]
Surface acoustic wave (SAW)	ZnO/SiO_2/Si SAW	0.02–2x10^6	–	[58]
Conductometric	Organic/inorganic hybrid membrane functionalized interface	25–400	5	[20]
Electrochemical	Gold nanoparticles (AuNPs)-polydopamine modified ITO electrode	4–800	1	[59]
Electro-chemiluminescence	Graphene oxide nanosheet/PAN nanowires CdSe quantum dots	0.5–10 × 10^3	0.17	[60]
Field effect transistor (FET) sensor	GO modified FET	4.7–300	1.53	[19]
Electrochemical	AuNPs and aptamer modified gold electrode	0.02–20	0.02	[24]
Electrochemical	Polypyrolle and AuNPs modified screen-printed graphite electrode	1–15 × 10^6	0.33	[61]
Lateral flow immunoassay (LFA)	Europium nanoparticles modified LFA	2–500	0.37	[16]
Optic	Aminopropyltriethoxysilane modified fiber optic	0.4–400	0.1	[21]
Electrochemical	SWCNTs modified pencil graphite electrode	0.5–30	0.5	[62]
Electrochemical	PPCE/IL 6 receptor modified ITO electrode	0.02–16	0.006	This study
Colorimetric	ELISA kit	10.24–400	1	[63]
Colorimetric	ELISA kit	15.6–1000	5	[64]
Colorimetric	ELISA kit	3–1000	3	[65]

B) Before antigen IL 6 (0.5 pg/mL) addition				After antigen IL 6 (0.5 pg/mL) addition				
Sample	Found by proposed immunosensor (pg/mL)	Standard Deviation	Coefficient Variation (%)	Total found by proposed immunosensor	Standard Deviation	Coefficient Variation (%)	Recovery (%)	Relative difference (%)
1	1.20	0.04	3.54	1.73	0.04	2.23	101,25	1,25
1	1.27			1.78			100,84	0,84
2	1.63	0.07	3.85	2.13	0.06	2.65	100,08	0,08
2	1.72			2.21			99,64	−0,36
3	0.97	0.04	4.17	1.48	0.04	2.54	100,56	0,56
3	0.91			1.42			100,82	0,82
4	1.92	0.05	2.48	2.42	0.05	1.88	100,21	0,21
4	1.99			2.49			100,07	0,07
5	3.82	0.04	0.90	4.20	0.07	1.63	97,10	−2,90
5	3.87			4.30			98,25	−1,75

3.7. Repeatability, reproducibility, reusability, storage stability and selectivity of the immunosensor

Repeatability and reproducibility are two important properties that show the analytical success of the biosensor. Therefore, the repeatability and reproducibility of the proposed biosensor were tested. To test the repeatability, 20 different bioelectrodes prepared on the same day were used for measurement of IL 6 antigen (1 pg/mL) and the proposed immunosensor had a relative standard deviation (RSD) of 2.82%. The low RSD value showed that the immunosensor had an acceptable repeatability. The impedimetric responses of 10 different immunosensors fabricated in the same conditions had a RSD value of 1.01%, which illustrated the excellent reproducibility of the biosensor fabrication protocol and the impedimetric detection (Fig. 5A).

Selectivity of the proposed immunosensor is also particularly significant in the biomarker analysis. To test the selectivity of the immunosensor, two different ITO/PPCE/IL 6R/BSA bioelectrodes were dipped in PBS solution containing interference protein biomarkers (VEGF, IL 1β, p53 and IL 8) with IL 6 antigen and only protein biomarkers (VEGF, IL 1β, p53 and IL 8), respectively. The concentrations of these biomarkers were 100 times higher than IL 6 biomarker concentration. Fig. 5B shows the selectivity result of the immunosensor. The immunosensor gave a small signal in the presence of other biomarkers and in the absence of IL 6 biomarker. In the presence of IL 6 and other biomarkers, the immunosensor gave response, that demonstrated the specificity of the biosensor for the detection of IL 6 antigen (Fig. 5B).

To investigate whether the biosensor can be reused, the working electrode immobilized with IL 6 antigen (ITO/PPCE/IL 6R/BSA/IL 6) was immersed in acidic solution (10 mM HCl) for 5 min and then, it was rinsed with ultrapure water and used again for measurement. As shown in Fig. 5C, at first, a small decrease in electrochemical signal was observed. After repetition of regeneration cycles, electrochemical signals were decreased obviously. The proposed immunosensor was reused at least 7 times, and the electrochemical signal diminished to 66.67% of the initial response at the end of the seventh measurement (Fig. 5C).

Another important feature of a good biosensor is long storage-stability. Seven different bioelectrodes prepared on the same day were used for IL 6 antigen detection in every week and no activity loss were obtained after 2 weeks. The bioelectrodes were stored at 4 °C when not in use. After 7 weeks of storage, the immunosensor retained 86.1% of its initial impedimetric response. Covalent binding between receptor and interface polymer provided a stable and long life immunosensor with a high sensitivity. Furthermore, its long storage life proved that there was no receptor denaturation on the electrode surface and the interface polymer matrix provided a biocompatible microenvironment for receptor. Fig. 5D illustrates an acceptable storage stability of the immunosensor and the proposed immunosensor allowed accurate determination of IL 6 biomarker during at least 7 weeks.

3.8. Determination of IL 6 antigen in human serum samples

The applicability of the fabricated immunosensor was evaluated by measurement of IL 6 antigen in human serum samples. Before analyzing these samples, they were diluted 10 times by using PBS buffer (pH 7.4). Then, the IL 6 antigen concentration in diluted human serum samples were measured by the constructed immunosensor. In order to evaluate the accuracy of the new biosensor, standard addition technique was used. The prepared ITO/PPCE/IL 6R/BSA electrodes were incubated in human serum and IL 6 antigen standard added human serum solutions

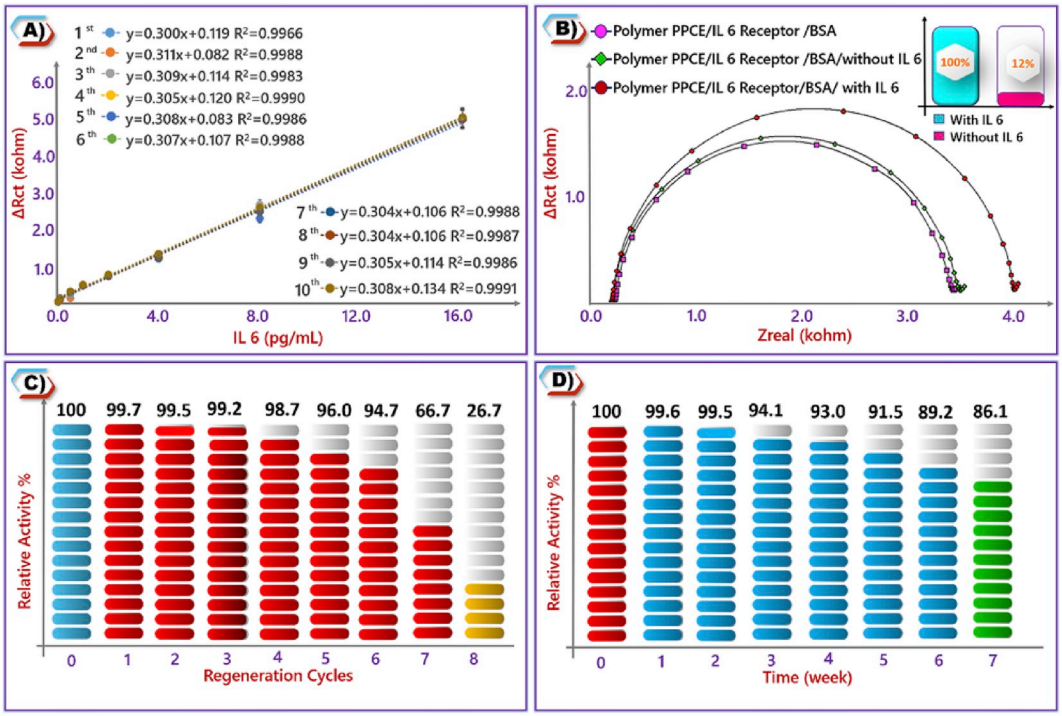

Fig. 5. Results of reproducibility (A), selectivity (B), regeneration (C) and storage stability (D).

for 30 min. Then, the impedimetric responses were measured and recovery yields were calculated. The results of real human samples analyses are illustrated in Table 1B. As seen in Table 1B, the designed biosensor displayed a good detection property with low LOD. In addition, the designed immunosensor could be potentially utilized in clinical analyses to determine the amount of IL 6 biomarker in human serum.

4. Conclusion

This study reported a novel, sensitive and label-free immunosensor for the impedimetric detection of IL 6, a biomarker of prostate cancer. Herein, PCE monomer was electropolymerized for the first time on the disposable ITO electrode to immobilize the IL 6 receptors. In this study, ITO electrodes were used for the fabrication of the immunosensor, because these electrodes were small, cheap and disposable. The PPCE polymer layer was constructed on ITO electrode by electropolymerization of PCE monomer. The formation of the polymer film was confirmed by SEM-EDX, FTIR, Raman analyses, and CV, EIS, SEM and AFM were used to show the differences formed during the biosensor fabrication. The PPCE polymer on the ITO electrode formed a large surface area for biomolecule immobilization and it improved the sensitivity of the biosensor. Furthermore, the usage of conjugated polymer was a contributing factor to increase the biosensor performance. The designed biosensor illustrated a detection limit of 6.0 fg/mL over the range of 0 0.02 pg/mL to 16 pg/mL IL6 concentration. The immunosensor was successfully applied to the analysis of IL 6 in human serum samples, showing good sensitivity and selectivity and presenting similar or better performance than other biosensors found in the literature. Besides, the unique characteristics of the PPCE polymer led to robustness, long-term storage stability and potential re-usability of the fabricated immunosensor. In conclusion, the developed biosensor provided a new strategy for label-free, rapid, simple and cost-effective detection of IL 6 biomarker.

CRediT author statement

Elif Burcu Aydın: Monomer synthesis, monomer electropolymerization, structures characterization, Methodology, biosensor fabrication, electrochemical measurements, morphological measurements, Software, writing.

Declaration of competing interest

The authors declare that they have no known competing financial interests or personal relationships that could have appeared to influence the work reported in this paper.

Appendix A. Supplementary data

Supplementary data to this article can be found online at https://doi.org/10.1016/j.talanta.2020.120909.

References

[1] S. Singh, A.A.S. Gill, M. Nlooto, R. Karpoormath, Prostate cancer biomarkers detection using nanoparticles based electrochemical biosensors, Biosens. Bioelectron. 137 (2019) 213–221, https://doi.org/10.1016/j.bios.2019.03.065.
[2] P. Sarkar, P.S. Pal, D. Ghosh, S.J. Setford, I.E. Tothill, Amperometric biosensors for detection of the prostate cancer marker (PSA), Int J Pharm 238 (1–2) (2002) 1–9, https://doi.org/10.1016/s0378-5173(02)00015-7.
[3] C.O. Madu, Y. Lu, Novel diagnostic biomarkers for prostate cancer, J. Canc. 1 (2010) 150–177, https://doi.org/10.7150/jca.1.150.
[4] S. McGrath, D. Christidis, M. Perera, S.K. Hong, T. Manning, I. Vela, N. Lawrentschuk, Prostate cancer biomarkers: are we hitting the mark? Prostate international 4 (4) (2016) 130–135, https://doi.org/10.1016/j.prnil.2016.07.002.
[5] J.R. Otero, B.G. Gomez, F.C. Juanatey, K.A. Touijer, Prostate Cancer Biomarkers: an Update, Urologic Oncology: Seminars and Original Investigations, Elsevier, 2014, pp. 252–260.
[6] A. Khanmohammadi, A. Aghaie, E. Vahedi, A. Qazvini, M. Ghanei, A. Afkhami, A. Hajian, H. Bagheri, Electrochemical biosensors for the detection of lung cancer biomarkers: a review, Talanta (2019) 120251.
[7] J. Tost, DNA methylation: an introduction to the biology and the disease-associated changes of a promising biomarker, Mol. Biotechnol. 44 (1) (2010) 71–81, https://doi.org/10.1007/s12033-009-9216-2.
[8] S. Dijkstra, P.F.A. Mulders, J.A. Schalken, Clinical use of novel urine and blood based prostate cancer biomarkers: a review, Clin. Biochem. 47 (10–11) (2014)

889–896, https://doi.org/10.1016/j.clinbiochem.2013.10.023.
[9] C. Stephan, B. Ralla, K. Jung, Prostate-specific antigen and other serum and urine markers in prostate cancer, Biochim. Biophys. Acta 1846 (1) (2014) 99–112, https://doi.org/10.1016/j.bbcan.2014.04.001.
[10] D. Wu, J. Ni, J. Beretov, P. Cozzi, M. Willcox, V. Wasinger, B. Walsh, P. Graham, Y. Li, Urinary biomarkers in prostate cancer detection and monitoring progression, Crit. Rev. Oncol. Hematol. 118 (2017) 15–26, https://doi.org/10.1016/j.critrevonc.2017.08.002.
[11] L.H. Pan, S.H. Kuo, T.Y. Lin, C.W. Lin, P.Y. Fang, H.W. Yang, An electrochemical biosensor to simultaneously detect VEGF and PSA for early prostate cancer diagnosis based on graphene oxide/ssDNA/PLLA nanoparticles, Biosens. Bioelectron. 89 (2017) 598–605, https://doi.org/10.1016/j.bios.2016.01.077.
[12] M. Schipper, G. Wang, N. Giles, J. Ohrnberger, Novel prostate cancer biomarkers derived from autoantibody signatures, Transl Oncol 8 (2) (2015) 106–111, https://doi.org/10.1016/j.tranon.2015.02.003.
[13] D.N. Patel, S.J. Freedland, New Prostate Cancer Biomarkers: the Search Continues vol. 211, ELSEVIER SCIENCE BV PO BOX, AMSTERDAM, NETHERLANDS, 2017, p. 1000.
[14] P. Karami, H. Bagheri, M. Johari-Ahar, H. Khoshsafar, F. Arduini, A. Afkhami, Dual-modality impedimetric immunosensor for early detection of prostate-specific antigen and myoglobin markers based on antibody-molecularly imprinted polymer, Talanta 202 (2019) 111–122.
[15] Y. Wang, J. Sun, Y. Hou, C. Zhang, D. Li, H. Li, M. Yang, C. Fan, B. Sun, A SERS-based lateral flow assay biosensor for quantitative and ultrasensitive detection of interleukin-6 in unprocessed whole blood, Biosens. Bioelectron. 141 (2019) 111432, https://doi.org/10.1016/j.bios.2019.111432.
[16] M. Tertis, P.I. Leva, D. Bogdan, M. Suciu, F. Graur, C. Cristea, Impedimetric aptasensor for the label-free and selective detection of Interleukin-6 for colorectal cancer screening, Biosens. Bioelectron. 137 (2019) 123–132 0.1016/j.bios.2019.05.012.
[17] D. Huang, H. Ying, D. Jiang, F. Liu, Y. Tian, C. Du, L. Zhang, X. Pu, Rapid and sensitive detection of interleukin-6 in serum via time-resolved lateral flow immunoassay, Anal. Biochem. 588 (2020) 113468, https://doi.org/10.1016/j.ab.2019.113468.
[18] T.H. Chou, C.Y. Chuang, C.M. Wu, Quantification of Interleukin-6 in cell culture medium using surface plasmon resonance biosensors, Cytokine 51 (1) (2010) 107–111, https://doi.org/10.1016/j.cyto.2010.04.004.
[19] J.F. Huang, H. Chen, W.B. Niu, D.W.H. Fam, A. Palaniappan, M. Larisika, S.H. Faulkner, C. Nowak, M.A. Nimmo, B. Liedberg, A.I.Y. Tok, Highly manufacturable graphene oxide biosensor for sensitive Interleukin-6 detection, RSC Adv. 5 (49) (2015) 39245–39251, https://doi.org/10.1039/c5ra05854f.
[20] K.Z. Liang, J.S. Qi, W.J. Mu, Z.X. Liu, Conductometric immunoassay for interleukin-6 in human serum based on organic/inorganic hybrid membrane-functionalized interface, Bioproc. Biosyst. Eng. 32 (3) (2009) 353–359, https://doi.org/10.1007/s00449-008-0254-0.
[21] K. Zhang, G. Liu, E.M. Goldys, Robust immunosensing system based on biotin-streptavidin coupling for spatially localized femtogram mL− 1 level detection of interleukin-6, Biosens. Bioelectron. 102 (2018) 80–86, https://doi.org/10.1016/j.bios.2017.11.023.
[22] G.C. Fan, X.L. Ren, C. Zhu, J.R. Zhang, J.J. Zhu, A new signal amplification strategy of photoelectrochemical immunoassay for highly sensitive interleukin-6 detection based on TiO2/CdS/CdSe dual co-sensitized structure, Biosens. Bioelectron. 59 (2014) 45–53, https://doi.org/10.1016/j.bios.2014.03.011.
[23] G.A. Messina, N.V. Panini, N.A. Martinez, J. Raba, Microfluidic immunosensor design for the quantification of interleukin-6 in human serum samples, Anal. Biochem. 380 (2) (2008) 262–267, https://doi.org/10.1016/j.ab.2008.05.055.
[24] L.S.S. Kumar, X. Wang, J. Hagen, R. Naik, I. Papautsky, J. Heikenfeld, Label free nano-aptasensor for interleukin-6 in protein-dilute bio fluids such as sweat, Analytical Methods 8 (17) (2016) 3440–3444, https://doi.org/10.1039/c6ay00331a.
[25] J. Tian, J. Huang, Y. Zhao, S. Zhao, Electrochemical immunosensor for prostate-specific antigen using a glassy carbon electrode modified with a nanocomposite containing gold nanoparticles supported with starch-functionalized multi-walled carbon nanotubes, Microchimica Acta 178 (1–2) (2012) 81–88.
[26] S. Ji, M. Lee, D. Kim, Detection of early stage prostate cancer by using a simple carbon nanotube@paper biosensor, Biosens. Bioelectron. 102 (2018) 345–350, https://doi.org/10.1016/j.bios.2017.11.035.
[27] A. Facchetti, π-Conjugated polymers for organic electronics and photovoltaic cell applications, Chem. Mater. 23 (3) (2010) 733–758, https://doi.org/10.1021/cm102419z.
[28] M. Gerard, A. Chaubey, B.D. Malhotra, Application of conducting polymers to biosensors, Biosens. Bioelectron. 17 (5) (2002) 345–359, https://doi.org/10.1016/s0956-5663(01)00312-8.
[29] B.D. Malhotra, A. Chaubey, S.P. Singh, Prospects of conducting polymers in biosensors, Anal. Chim. Acta 578 (1) (2006) 59–74, https://doi.org/10.1016/j.aca.2006.04.055.
[30] F.R.R. Teles, L.R. Fonseca, Applications of polymers for biomolecule immobilization in electrochemical biosensors, Mat Sci Eng C-Bio S 28 (8) (2008) 1530–1543, https://doi.org/10.1016/j.msec.2008.04.010.
[31] A. Ramanavičius, A. Ramanavičienė, A. Malinauskas, Electrochemical sensors based on conducting polymer—polypyrrole, Electrochim. Acta 51 (27) (2006) 6025–6037, https://doi.org/10.1016/j.electacta.2005.11.052.
[32] M. Singh, P.K. Kathuroju, N. Jampana, Polypyrrole based amperometric glucose biosensors, Sensor. Actuator. B Chem. 143 (1) (2009) 430–443, https://doi.org/10.1016/j.snb.2009.09.005.
[33] J. Njagi, S. Andreescu, Stable enzyme biosensors based on chemically synthesized Au–polypyrrole nanocomposites, Biosens. Bioelectron. 23 (2) (2007) 168–175, https://doi.org/10.1016/j.bios.2007.03.028.
[34] J. Wang, M. Musameh, Carbon-nanotubes doped polypyrrole glucose biosensor, Anal. Chim. Acta 539 (1–2) (2005) 209–213, https://doi.org/10.1016/j.aca.2005.02.059.
[35] L.T. Truong, M. Chikae, Y. Ukita, Y. Takamura, Labelless impedance immunosensor based on polypyrrole–pyrolecarboxylic acid copolymer for hCG detection, Talanta 85 (5) (2011) 2576–2580, https://doi.org/10.1016/j.talanta.2011.08.018.
[36] G.F. Cheng, J. Zhao, Y.H. Tu, P.A. He, Y.H. Fang, A sensitive DNA electrochemical biosensor based on magnetite with a glassy carbon electrode modified by mutiwalled carbon nanotubes in polypyrrole, Anal. Chim. Acta 533 (1) (2005) 11–16, https://doi.org/10.1016/j.aca.2004.10.044.
[37] C.M. Li, C.Q. Sun, S. Song, V.E. Choong, G. Maracas, X.J. Zhang, Impedance labelless detection-based polypyrrole DNA biosensor, Front. Biosci. 10 (2005) 180–186, https://doi.org/10.2741/1519.
[38] W. Khan, M. Kapoor, N. Kumar, Covalent attachment of proteins to functionalized polypyrrole-coated metallic surfaces for improved biocompatibility, Acta Biomater. 3 (4) (2007) 541–549, https://doi.org/10.1016/j.actbio.2007.01.006.
[39] S. Maeda, R. Corradi, S.P. Armes, Synthesis and characterization of carboxylic acid-functionalized polypyrrole-silica microparticles, Macromolecules 28 (8) (1995) 2905–2911, https://doi.org/10.1021/ma00112a042.
[40] M. Aydın, A sensitive and selective approach for detection of IL 1α cancer biomarker using disposable ITO electrode modified with epoxy-substituted polythiophene polymer, Biosens. Bioelectron. (2019) 111675, https://doi.org/10.1016/j.bios.2019.111675.
[41] G.E. Tranter, Protein structure analysis by CD, FTIR, and Raman spectroscopies, third ed., Encyclopedia of Spectroscopy and Spectrometry vol. 3, N-R, 2017, pp. 740–758, https://doi.org/10.1016/B978-0-12-409547-2.12099-2.
[42] E.B. Aydın, M. Aydın, M.K. Sezgintürk, Selective and ultrasensitive electrochemical immunosensing of NSE cancer biomarker in human serum using epoxy-substituted poly (pyrrole) polymer modified disposable ITO electrode, Sensor. Actuator. B Chem. (2019) 127613, https://doi.org/10.1016/j.snb.2019.127613.
[43] A. Ghosh, S. Raha, S. Dey, K. Chatterjee, A.R. Chowdhury, A. Barui, Chemometric analysis of integrated FTIR and Raman spectra obtained by non-invasive exfoliative cytology for the screening of oral cancer, Analyst 144 (4) (2019) 1309–1325, https://doi.org/10.1039/c8an02092b.
[44] M.T. Alula, Z.T. Mengesha, E. Mwenesongole, Advances in surface-enhanced Raman spectroscopy for analysis of pharmaceuticals: a review, Vib. Spectrosc. 98 (2018) 50–63, https://doi.org/10.1016/j.vibspec.2018.06.013.
[45] D. Kurouski, R.P. Van Duyne, I.K. Lednev, Exploring the structure and formation mechanism of amyloid fibrils by Raman spectroscopy: a review, Analyst 140 (15) (2015) 4967–4980, https://doi.org/10.1039/c5an00342c.
[46] M. Aydın, E.B. Aydın, M.K. Sezgintürk, A highly selective electrochemical immunosensor based on Conductive Carbon Black and Star PGMA polymer composite material for IL-8 biomarker detection in human serum and saliva, Biosens. Bioelectron. (2018), https://doi.org/10.1016/j.bios.2018.07.010.
[47] L.A. Austin, S. Osseiran, C.L. Evans, Raman technologies in cancer diagnostics, Analyst 141 (2) (2016) 476–503, https://doi.org/10.1039/c5an01786f.
[48] T. Kitagawa, S. Hirota, Raman Spectroscopy of Proteins Handbook of Vibrational Spectroscopy, Wiley, New York, 2006.
[49] I. Bruzas, W. Lum, Z. Gorunmez, L. Sagle, Advances in surface-enhanced Raman spectroscopy (SERS) substrates for lipid and protein characterization: sensing and beyond, Analyst 143 (17) (2018) 3990–4008, https://doi.org/10.1039/c8an00606g.
[50] A. Bonifacio, C. Beleites, F. Vittur, E. Marsich, S. Semeraro, S. Paoletti, V. Sergo, Chemical imaging of articular cartilage sections with Raman mapping, employing uni- and multi-variate methods for data analysis, Analyst 135 (12) (2010) 3193–3204, https://doi.org/10.1039/c0an00459f.
[51] E.B. Aydın, M. Aydın, M.K. Sezgintürk, Ultrasensitive determination of cadherin-like protein 22 with A label-free electrochemical immunosensor using brush type poly (thiophene-g-glycidylmethacrylate) modified disposable ITO electrode, Talanta (2019), https://doi.org/10.1016/j.talanta.2019.03.082.
[52] M. Aydın, E.B. Aydın, M.K.J.B. Sezgintürk, Bioelectronics, Electrochemical immunosensor for CDH22 biomarker based on benzaldehyde substituted poly (phosphazene) modified disposable ITO electrode, A new fabrication strategy for biosensors 126 (2019) 230–239, https://doi.org/10.1016/j.bios.2018.10.051.
[53] Y. Chen, B. Jiang, Y. Xiang, Y. Chai, R. Yuan, Target recycling amplification for sensitive and label-free impedimetric genosensing based on hairpin DNA and graphene/Au nanocomposites, Chem. Commun. 47 (48) (2011) 12798–12800, https://doi.org/10.1039/c1cc14902d.
[54] E.B. Aydin, A label-free and sensitive impedimetric immunosensor for TNF? biomarker detection based on epoxysilane-modified disposable ITO-PET electrode, Int. J. Environ. Anal. Chem. (2019), https://doi.org/10.1080/03067319.2019.1679807.
[55] E.B. Aydın, M.K. Sezgintürk, A sensitive and disposable electrochemical immunosensor for detection of SOX2, a biomarker of cancer, Talanta 172 (2017) 162–170, https://doi.org/10.1016/j.talanta.2017.05.048.
[56] M. Aydın, E.B. Aydın, M.K. Sezgintürk, A highly selective poly (thiophene)-graft-Poly (methacrylamide) polymer modified ITO electrode for neuron specific enolase detection in human serum, Macromol. Biosci. (2019) 1900109, https://doi.org/10.1002/mabi.201900109.
[57] T. Yang, S. Wang, H.L. Jin, W.W. Bao, S.M. Huang, J.C. Wang, An electrochemical impedance sensor for the label-free ultrasensitive detection of interleukin-6 antigen, Sensor. Actuator. B Chem. 178 (2013) 310–315, https://doi.org/10.1016/j.snb.2012.12.107.
[58] S. Krishnamoorthy, A.A. Iliadis, T. Bei, G.P. Chrousos, An interleukin-6 ZnO/SiO2/

Si surface acoustic wave biosensor, Biosens. Bioelectron. 24 (2) (2008) 313–318, https://doi.org/10.1016/j.bios.2008.04.011.
[59] G. Wang, H. Huang, G. Zhang, X. Zhang, B. Fang, L. Wang, Dual amplification strategy for the fabrication of highly sensitive interleukin-6 amperometric immunosensor based on poly-dopamine, Langmuir 27 (3) (2011) 1224–1231, https://doi.org/10.1021/la1033433.
[60] P.Z. Liu, X.W. Hu, C.J. Mao, H.L. Niu, J.M. Song, B.K. Jin, S.Y. Zhang, Electrochemiluminescence immunosensor based on graphene oxide nanosheets/polyaniline nanowires/CdSe quantum dots nanocomposites for ultrasensitive determination of human interleukin-6, Electrochim. Acta 113 (2013) 176–180, https://doi.org/10.1016/j.electacta.2013.09.074.
[61] M. Tertis, B. Ciui, M. Suciu, R. Sandulescu, C. Cristea, Label-free electrochemical aptasensor based on gold and polypyrrole nanoparticles for interleukin 6 detection, Electrochim. Acta 258 (2017) 1208–1218, https://doi.org/10.1016/j.electacta.2017.11.176.
[62] R. Malhotra, V. Patel, J.P. Vaque, J.S. Gutkind, J.F. Rusling, Ultrasensitive electrochemical immunosensor for oral cancer biomarker IL-6 using carbon nanotube forest electrodes and multilabel amplification, Anal. Chem. 82 (8) (2010) 3118–3123, https://doi.org/10.1021/ac902802b.
[63] https://www.thermofisher.com/elisa/product/IL-6-Human-ELISA-Kit/EH2IL6.
[64] https://www.mybiosource.com/human-elisa-kits/interleukin-6-il-6/261259.
[65] https://www.raybiotech.com/human-il6-elisa-kit/.